Transient Model and Simulation of a Single Effect Water/Lithium-Bromide Vapour Absorption System

D.H. Jeggels, R.T. Dobson

Department of Mechanical and Mechatronic Engineering, Stellenbosch University, Private Bag X1, Matieland, 7602, South Africa

Abstract

This paper presents a model for the transient and dynamic modelling of a single-effect lithium-bromide/water vapour absorption refrigeration system. The basis for the model is the application of the principles of mass conservation and energy conservation to the internal refrigerant and solution control volumes. External heating and cooling streams are defined through inlet conditions, heat exchanger fluid mass volumes and an overall heat transfer coefficient values. A refrigeration load is modelled by a large mass of water external to the vapour absorption system. Results obtained from the simulation model are discussed for a constant temperature heating stream.

Keywords: vapour absorption, transient simulation, LiBr/water

1. Introduction

The start up behaviour and system response to varying external interfaces of a vapour absorption system is of interest to the further development and improvement of vapour absorption applications in dynamic environments. This is relevant when the energy supplied to the system and the load on the system can fluctuate. It is also of interest when incorporating vapour absorption refrigeration systems into larger installations where the behaviour and response of a vapour absorption system is dependant on the interfaces of the larger system such as in a solar powered refrigeration plant, a waste heat recovery process or a combined heating and power installation.

Email address: rtd@sun.ac.za (R.T. Dobson)

Nomenclature

Variables		*Component Subscripts*	
A	Area (m^2)	A	Absorber
C	Concentration (kg kg^{-1})	E	Evaporator
c	Specific heat capacity (J kg^{-1} K^{-1})	EA	Evaporator-absorber vessel
E	Energy (J)	C	Condenser
h	Enthalpy (J kg^{-1})	f	Liquid film
m	Mass (kg)	G	Generator
$\dot{m}$	Mass flow rate (kg s^{-1})	GC	Generator-condenser vessels
P	Pressure (Pa)	L	Evaporator load
$\dot{Q}$	Rate of heat transfer (J s^{-1})	p	Liquid pool
T	Temperature (K)	S	Solution heat exchanger
t	Time (s)		
UA	Overall heat transfer coefficient (W K^{-1})	*Fluid Subscripts*	
V	Volume (m^3)	l	Liquid refrigerant
ρ	Density (kg m^{-3})	v	Vapour refrigerant
Stream Subscripts		*Stream Subscripts*	
cw	Cooling water	$cond$	Condensation
hw	Heating water	o	Outlet condition

The last two decades has seen a number approaches used to describe and model the behaviour of a vapour absorption system. Herold et al. [1] discusses how the Engineering Equation Solver (EES) can be used to simultaneously solve the heat transfer rates, heat transfer surface areas and cycle temperatures from supplied external cycle temperature in combination with the values for the overall heat transfer coefficient values in a steady state scenario. EES is also used in an extension of this example to maximize the refrigeration potential that can be obtained from the cycle specifications. Grossman and Zaltash [2] discusses the development and usage of the ABsorption SIMulation (ABSIM) software package. This simulation program was made for the sole purpose of steady state simulation of vapour absorption cycles and makes use of a graphical user interface that allows a user to configure the cycle components that are to be simulated. ABSIM is capable of simulating expansive vapour absorption cycles and includes the property functions for a number of vapour absorption working pairs. Somers et al. [3] made use of ASPEN Plus, a chemical process package, to simulate both a single effect and a double effect vapour absorption cycle. The results of this

simulation compared well with the results obtained from a similar simulation that was performed with EES. Bakhtiari et al. [4] developed a model to assess the steady state behaviour of a single effect water/lithium-bromide cycle. The external streams were used as the user specifications for this steady state simulation. Results from an experimental apparatus were used for verification of the model and the results were favourable.

Kohlenbach and Ziegler [5, 6] combined the use of a steady state solution with a transient model in order to examine the dynamic response of a water/lithium-bromide cycle. A finite difference Jacobian method was used to solve the equations via MATLAB®. Kim and Park [7] implemented differential equations in order to describe the transient behaviour and dynamic response of a single effect ammonia/water absorption chiller. A Runge-Kutta-Merson technique was used to simultaneously solve the various equations. The behaviour of the simulated cycle during transient start-up as well as during a dynamic response to a change in the fuel supply of the cycle was discussed.

Shin et al. [8] discusses the modelling of a double-effect lithium-bromide/water absorption chiller. The core components of two generators, condenser, absorber and evaporator of the model were modelled with shell-tube heat exchangers. Simulation results were compared with a direct-fired commercial double-effect absorption chiller with results after roughly 80 minutes of operation comparing well.

Evola et al. [9] presented a mathematical model for the dynamic simulation of a lithium-bromide/water absorption chiller. The presented model applied mass and energy balances to the internal vapour absorption components. Verification of the model is made by comparison with experimental results obtained from a solar powered Rotartica absorption chiller. The experimental and theoretical results compare very well.

The model presented in this article is similar to that presented by Evola et al. [9]. However, the extent to which the models are similar could not be examined in greater detail as the specifics concerning the way in which Evola et al. [9] dealt with the desorption of vapour refrigerant in the generator and the absorption of vapour refrigerant in the absorber is not disclosed.

2. Description of the Model

Figure 1 shows the chosen model for the single-effect lithium-bromide system. The generator and condenser share a single vessel and have a com-

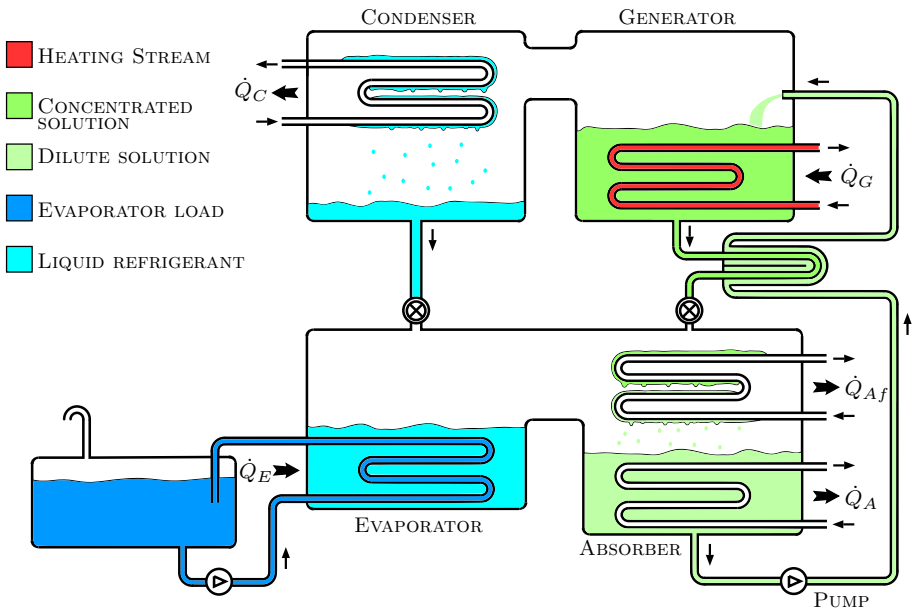

Figure 1: Schematic of chosen single-effect vapour absorption refrigeration system

mon vapour space with the generator heat exchanger located in a pool of lithium-bromide/water solution and the condenser heat exchanger providing a surface condensation of the refrigerant vapour. Similarly, the evaporator and absorber share a single vessel with a common vapour space. Two vapour-liquid absorption surfaces are including in the absorber section of the model. The solution return from the generator to the absorber forms the first vapour-liquid interface on a heat exchanger in the absorber and the second vapour-liquid interface is the surface of the solution pool.

A number of assumptions were made to in order to simplify the transition to a mathematical formulation of the model. The most notable of these assumptions are:

- the generator solution and the generator-condenser vapour space is combined with regard to the conservation of mass and energy
- the generator solution saturation pressure and the shared vapour space pressure are the same
- the generator-condenser vapour is at a temperature between the generator solution temperature and the vapour saturation temperatures

- the evaporator liquid and vapour are combined with regard to the conversation of mass and energy
- the evaporator liquid and vapour are always at the same saturated pressure and temperature state
- vapour absorption is described by a mass convection approach

These assumptions make it possible to reduce the number of independent variables in the numerical simulation. Furthermore, these assumptions eliminate the need to determine the behaviour of the vapour-liquid interfaces in the desorption of vapour from generator solution to high pressure vapour space and the evaporation of refrigerant from the evaporator liquid to the low pressure vapour space.

The remainder of the assumptions that were made are similar to those made by Kohlenbach and Ziegler [5, 6] and Evola et al. [9]:

- temperature, concentration and pressure is homogeneous inside each control volume
- refrigerant in the condenser and evaporator is pure
- no heat transfer to or from the surroundings
- no conductive, convective and radiative heat transfer between internal solution and refrigerant control volumes
- external streams are supplied at a constant temperature and mass flow rate
- all heat exchangers have constant overall heat transfer coefficients
- internal streams are at a constant mass flow rate
- pressure loss in the interconnecting pipework is ignored
- throttling valves are adiabatic
- fluid delay between internal components is neglected

Property equations for the solution of lithium-bromide/water were used from the work presented by Pátek and Klomfar [10, 11]. The properties of water were included by the works of Mills [12], Wagner et al.[13] and Çengel [14].

Combining the assumptions with the schematic representation of the model, Figure 1, resulted in the control volume representation of the model as seen in Figure 2. The interaction between the evaporator liquid and vapour control volume with the absorber pool and film is represented by the absorption of vapour to the film $\dot{m}_{absf}$, absorption of vapour to the pool $\dot{m}_{absp}$ and the overflow of liquid refrigerant from the evaporator pool to the absorber pool $\dot{m}_{Eo}$.

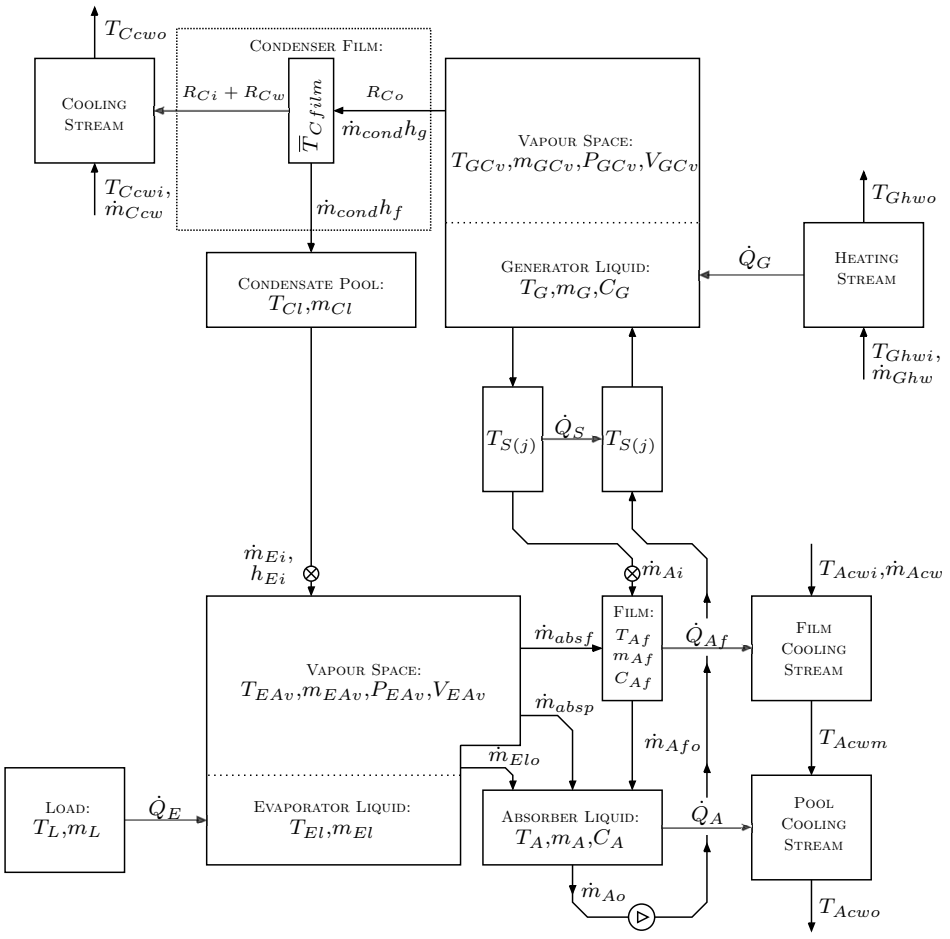

Figure 2: Control volumes for the theoretical model

Each of the heating and cooling streams that interact with the vapour absorption system are defined by the product of the respective overall heat transfer coefficient and the difference between the associated external stream

and internal control volume. While the formulation of the heat transfer rates is specified with a singular variable for the external streams, the external streams are divided into a number of sections along the length of each heat exchanger and the accumulative effect is represented by the total heat transfer rate.

$$\dot{Q}_G = UA_G(T_{Ghw} - T_G) \tag{1}$$
$$\dot{Q}_C = UA_C(T_{GCvsat} - T_{Ccw}) \tag{2}$$
$$\dot{Q}_E = UA_E(T_{Lhw} - T_E) \tag{3}$$
$$\dot{Q}_{Af} = UA_{Af}(T_{Af} - T_{Afcw}) \tag{4}$$
$$\dot{Q}_A = UA_A(T_A - T_{Acw}) \tag{5}$$
$$\dot{Q}_S = UA_S(T_{SGo} - T_{SGi}) \tag{6}$$

With regard to the heat transfer in the solution heat exchanger $\dot{Q}_S$ the heat exchanger was similarly divided into a number of sections along the length of the heat exchanger between the generator and absorber.

2.1. General Equations

The conservation of mass and energy was applied in a way that made it possible to determine the unknown conditions after a small time step has occurred. Two general equations were formulated on the basis of the conservation of mass, the first of which considers the total mass of a control volume:

$$\begin{aligned} \frac{\Delta m}{\Delta t} &= \sum \dot{m}_i - \sum \dot{m}_o \\ \frac{m^{t+\Delta t} - m^t}{\Delta t} &= \sum \dot{m}_i - \sum \dot{m}_o \\ m^{t+\Delta t} &= m^t + \Delta t \left(\sum \dot{m}_i - \sum \dot{m}_o \right) \end{aligned} \tag{7}$$

The second application of the conservation of mass considered the mass of salt absorbent in a control volume:

$$\begin{aligned}\frac{\Delta mC}{\Delta t} &= \sum \dot{m}_i C_i - \sum \dot{m}_o C_o \\ \frac{m^{t+\Delta t}C^{t+\Delta t} - m^t C^t}{\Delta t} &= \sum \dot{m}_i C_i - \sum \dot{m}_o C_o \\ C^{t+\Delta t} &= \frac{m^t C^t + \Delta t}{m^{t+\Delta t}} \Big(\sum \dot{m}_i C_o - \sum \dot{m}_o C_o \Big) \end{aligned} \tag{8}$$

An indirect method of determining the new temperature of a control volume was formulated from the conservation of mass:

$$\begin{aligned}\frac{\Delta E}{\Delta t} &= \sum \dot{E}_i - \sum \dot{E}_o \\ \frac{\Delta mh}{\Delta t} &= \sum \dot{Q}_i + \sum \dot{m}_i h_i - \sum \dot{Q}_o \\ &\quad - \sum \dot{m}_o h_o \\ h^{t+\Delta t} &= \frac{m^t h^t + \Delta t}{m^{t+\Delta t}} \Big(\sum \dot{Q}_i + \sum \dot{m}_i h_i \\ &\quad - \sum \dot{Q}_o - \sum \dot{m}_o h_o \Big) \end{aligned} \tag{9}$$

and the property equations of the relevant fluids. A direct method to determine the new temperature was used for the condenser and evaporator control volumes where the specific heat was included:

$$\begin{aligned} T^{t+\Delta t} = \frac{m^t c^t T^t + \Delta t}{m^{t+\Delta t} c^t} \Big(\sum \dot{Q}_i + \sum \dot{m}_i h_i \\ - \sum \dot{Q}_o - \sum \dot{m}_o h_o \Big) \end{aligned} \tag{10}$$

2.2. Generator and Condenser

The conservation of mass on the combined generator solution G and generator-condenser vapour GCv is described by the following equation:

$$\begin{aligned} m_G^{t+\Delta t} + m_{GCv}^{t+\Delta t} = m_G^t + m_{GCv}^t + \Delta t(\dot{m}_{Gi} \\ - \dot{m}_{Go} - \dot{m}_{cond}) \end{aligned} \tag{11}$$

where the mass of the vapour is the product of the volume and density of the vapour:

$$m_{GCv} = V_{GCv} \rho_v \{T_{GCv}, P_{GCv}\} \tag{12}$$

with the volume of the vapour calculated by subtracting the volume of the generator solution and condenser liquid from the total volume of the vessel:

$$V_{GCv} = V_{GC} - m_G/\rho_G - m_{Cl}/\rho_{Cl} \tag{13}$$

The conservation of mass applied with respect to the concentration in the generator gives the following equation:

$$C_G^{t+\Delta t} = \frac{m_G^t C_G^t + \Delta t}{m_G^{t+\Delta t}}(\dot{m}_{Gi} C_{Gi} - \dot{m}_{Go} C_G) \tag{14}$$

The temperature of the vapour in the generator-condenser vessel was defined as a function of the generator solution temperature and the vapour saturation temperature:

$$T_{GCv} = T_{GCvsat} + 0.5(T_G - T_{GCvsat}) \tag{15}$$

Applying the conservation of energy to the same combined control volume:

$$\begin{aligned} &m_G^{t+\Delta t} h_G^{t+\Delta t} + m_{GCv}^{t+\Delta t} h_{GCv}^{t+\Delta t} = m_G^t h_G^t \\ &+ m_{GCv}^t h_{GCv}^t + \Delta t(\dot{m}_{Gi} h_{Gi} - \dot{m}_{Go} h_G \\ &- \dot{m}_{cond} h_{GCv}) \end{aligned} \tag{16}$$

makes it possible to iteratively determine the new generator temperature and concentration by combining Equations 11 to 16

The updated conditions for the condenser liquid pool are calculated by application of the conservation of mass:

$$m_C^{t+\Delta t} = m_C^t + \Delta t(\dot{m}_{cond} - \dot{m}_{Co}) \tag{17}$$

and the conservation of energy:

$$\begin{aligned} T_C^{t+\Delta t} =& \frac{m_C^t c_C^t T_C^t + \Delta t}{m_C^{t+\Delta t} c_C^t}(\dot{m}_{cond} c_{Cf} T_{Cf} \\ &- \dot{m}_{Co} c_C T_C) \end{aligned} \tag{18}$$

where the rate of condensation is

$$\dot{m}_{cond} = \dot{Q}_C/(h_{GCv} - cT_{GCsat}) \tag{19}$$

2.3. Evaporator and Absorber

The mass of vapour in the evaporator-absorber vessel is determined in the following manner:

$$m_{EAv} = V_{EAv}\rho_v\{T_{GCv}, P_{GCv}\} \tag{20}$$

where the volume of the vapour is calculated by subtracting the volume of the absorber solution and the evaporator liquid from the total volume of the vessel:

$$V_{EAv} = V_{EA} - m_A/\rho_A - m_{El}/\rho_{El} \tag{21}$$

The rate of absorption was defined as a mass convection process where the driving potential behind the vapour-liquid interaction is the difference between the vapour pressure and the saturation pressure of the absorber solution interfaces:

$$\dot{m}_{abs} = h_{abs}A_{abs}(P_{EAv} - P_A) \tag{22}$$

The conservation of mass is applied to the evaporator control volume:

$$\begin{aligned} m_E^{t+\Delta t} + m_{EAv}^{t+\Delta t} &= m_E^t + m_{EAv}^t \\ &+ \Delta t(\dot{m}_{Ei} - \dot{m}_{absp} - \dot{m}_{absf} - \dot{m}_{Eo}) \end{aligned} \tag{23}$$

making it possible to calculated the new mass of liquid refrigerant when using Equation 23 with Equations 20 and 22 when applied to both of the absorber solution interfaces.

Completing the calculations regarding the evaporator control volume is performed by applying the conservation of energy:

$$\begin{aligned} &m_E^{t+\Delta t}c_E^t T_E^{t+\Delta t} + m_{EAv}^{t+\Delta t}h_{EAv}^{t+\Delta t} = m_E^t C_E^t T_E^t \\ &+ m_{EAv}^t h_{EAv}^t + \Delta t(\dot{m}_{Ei}c_{Ei}T_{Ei} - h_{EAv}(\dot{m}_{absp} \\ &+ \dot{m}_{absf}) - \dot{m}_{Eo}c_E T_E) \end{aligned} \tag{24}$$

that can be used to iteratively determine the new temperature of the evaporator vapour and liquid.

The conservation of mass is then applied to the solution in the absorber film and pool, as can be seen in Equations 25 to 28

$$m_{Af}^{t+\Delta t} = m_{Af}^{t} + \Delta t(\dot{m}_{Ai} + \dot{m}_{absf} - \dot{m}_{Afo}) \tag{25}$$

$$C_{Af}^{t+\Delta t} = \frac{m_{Af}^{t} C_{Af}^{t} + \Delta t}{m_{Af}^{t+\Delta t}}(\dot{m}_{Ai} C_{Ai} - \dot{m}_{Afo} C_{Af}) \tag{26}$$

$$m_{A}^{t+\Delta t} = m_{A}^{t} + \Delta t(\dot{m}_{Afo} + \dot{m}_{absp} + \dot{m}_{Eo} - \dot{m}_{Ao}) \tag{27}$$

$$C_{A}^{t+\Delta t} = \frac{m_{A}^{t} C_{A}^{t} + \Delta t}{m_{A}^{t+\Delta t}}(\dot{m}_{Afo} C_{Af} - \dot{m}_{Ao} C_{A}) \tag{28}$$

The conservation of energy is applied to the absorber solution control volumes:

$$h_{Af}^{t+\Delta t} = \frac{m_{Af}^{t} h_{Af}^{t} + \Delta t}{m_{Af}^{t+\Delta t}}(\dot{m}_{Ai} h_{Ai} + \dot{m}_{absf} h_{EAv} - \dot{m}_{Afo} h_{A}) \tag{29}$$

$$h_{A}^{t+\Delta t} = \frac{m_{A}^{t} h_{A}^{t} + \Delta t}{m_{A}^{t+\Delta t}}(\dot{m}_{Afo} h_{Af} + \dot{m}_{absp} h_{EAv} - \dot{m}_{Ao} h_{A}) \tag{30}$$

2.4. External Load

A mass of water external to the system is used to model a load on the vapour absorption system. The mass and circulation rate of this load is constant. Applying the conservation of energy to this external mass will update the temperature of the external mass in the following way:

$$\begin{aligned} m_L c(T_L^{t+\Delta t} - T_L^{t}) &= \Delta t(\dot{m}_L c T_{Lhwo} - \dot{m}_L c T_L) \\ T_L^{t+\Delta t} &= T_L^{t} + \Delta t \dot{m}_L / m_L (T_{Lhwo} - T_L) \end{aligned} \tag{31}$$

2.5. Vapour Absorption

There are many approaches that can be used to mathematically describe the combined heat and mass transfer vapour-liquid interaction in the evaporator and absorber. Killion and Garimella [15] reviewed numerous methods of modelling this interaction with many studies focusing on the

The method used in this model is based on mass convection and was chosen due to the way in which it can be incorporated into the theoretical model and simulation.

$$\dot{m}_{abs} = h_{abs} A_{abs}(P_{EA} - P_A) \tag{32}$$

3. Simulation Results

Results obtained from the completed vapour absorption cycle simulation can be seen in Figure 3. The simulated cycle successfully cooled the external load of 1000 kg from its initial temperature of 20 ℃ to a final temperature of 10 ℃ over a time span of three hours.

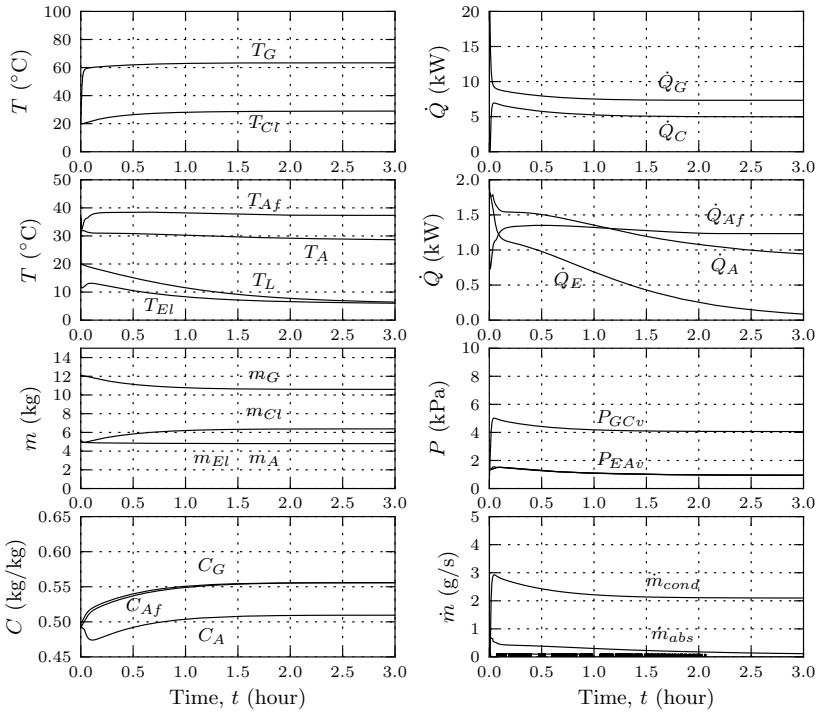

Figure 3: Results from theoretical model

Specifications for the theoretical model are listed in Tables 1, 2 and 3. Table 1 contains the specifications for the initial conditions for the internal control volumes in combination with the external streams that interact with the cycle:

Table 2 lists the internal and external specifications for the absorber-evaporator section of the complete cycle:

The mass flow rates for the internal streams are shown in Table 3. In

Table 1: Generator and condenser specifications for the complete vapour absorption cycle

Condenser Cooling Stream	
T_{Ccwi}	20 ℃
$\dot{m}_{Ccw}$	0.5 kg/s
k	18 W/(m ℃)
l	10.5 m
d_o	0.0127 m
t	0.0012 m

Common Vapour Space	
T_{GCv}	20 ℃
V_{GCt}	1.1 m^3
Condenser Liquid Pool	
T_{Cl}	20 ℃
m_{Cl}	5 kg

Generator Liquid Solution	
T_{Gl}	20 ℃
m_G	12 kg
C_G	0.5 kg/kg
Generator Heating Stream	
T_{Ghwi}	80 ℃
$\dot{m}_{Ghw}$	0.5 kg/s
UA_G	500 W/℃

Table 2: Absorber and evaporator variables for the simulation of the complete vapour absorption cycle

Evaporator Liquid Pool	
T_{El}	20 ℃
m_{El}	10 kg
Evaporator Load	
T_L	20 ℃
m_L	1000 kg
$\dot{m}_L$	0.5 kg/s
UA_E	250 W/℃

Common Vapour Space	
T_{EAv}	20 ℃
V_{EAv}	1.3m^3
Vapour-Liquid Interfaces	
k_{absf}	0.005
A_{absf}	0.64 m^2
k_{absp}	0.002
A_{absp}	0.25 m^2

Absorber Liquid Solution	
T_A	20 ℃
m_A	20 ℃
C_A	0.5 kg/kg
Absorber Film	
T_{Af}	20 ℃
V_{Af}	0.00127 m^3
C_{Af}	0.5 kg/kg

addition to internal flow rates this table also contains the time related specifications of the simulation.

Table 3: Inter-vessel stream, time and component specifications for the simulation of a complete vapour absorption

Condenser to Evaporator	
$\dot{m}_{Co}$	0.0021 kg/s
Time	
t_{end}	3 hours
Δt	0.01 s

Generator to Absorber	
$\dot{m}_{Go}$	0.0231 kg/s
Solution Heat Exchanger	
	active
UA_{SHX}	300 W/℃

Absorber to Generator	
$\dot{m}_{Gi}$	0.0252 kg/s
Absorber Vapour-Liquid Interfaces	
Pool	Cooling @ 25 ℃, 300 W/℃
Film	Active & Cooled @ 25 ℃, 100 W/℃

4. Validation

Figure 4 shows a comparison between the theoretical and experimental temperatures plotted for the duration of this test run. It can be seen that while the theoretical temperatures do not match the experimental results exactly, the overall tendency is captured remarkably well. In comparing the three data sets it was determined that the largest average difference and maximum difference in theoretical and experimental values is 3.50% for T_{GCv} and 23.0% for T_G. The difference in gradient that is seen in the rise from the initial conditions to the steady state conditions can be attributed to the sudden release of vapour from the generator's solution.

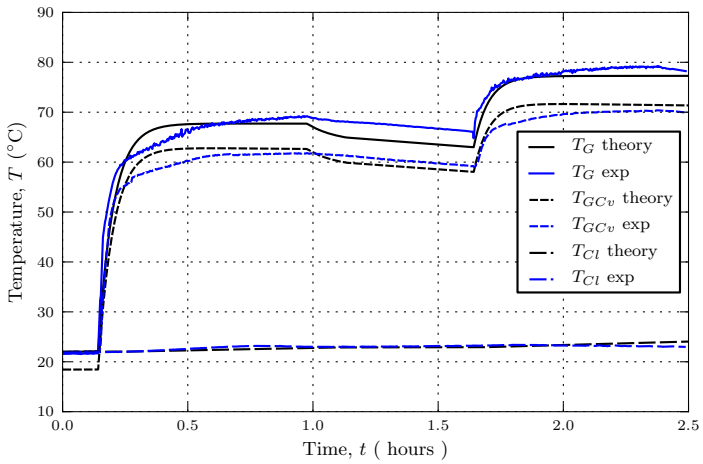

Figure 4: Comparison of experimental and theoretical results

Table 4 shows the initial conditions of the experimental apparatus in addition to the values of the external streams.

Table 4: Table 1: Specifications for comparison

Control Volume	Variable	Value
Generator Solution	T_G	22 °C
	m_G	20.8 kg
	C_G	0.384
Condensate Pool	T_{Cl}	22 °C
	m_{Cl}	9.17 kg
Vessel	V_T	0.11 m^3
	UA_{loss}	1.44 W/°C
Generator	$\dot{m}_{Ghw}$	0.45 kg/s
Heating Stream	T_{Ghwi}	70.3 °C[1]
	T_{Ghwi}	80.4 °C[2]
	UA_G	249.4 W/K
Condenser	$\dot{m}_{Ghw}$	0.26 kg/s
Cooling Stream	T_{Ccwi}	18.2 °C
	UA_C	11.9 W/K

1: between minute 8 and 58, 2: between minute 98 and 142

5. Conclusion

The extent to which the simulation models the behaviour of an actual vapour absorption cycle was not completely assessed as only preliminary results could be obtained from the experimental apparatus. What could be compared gave an indication of promising results in that the behaviour of the experimental apparatus was emulated to a reasonable degree, with the largest average difference in temperature for any set of experimental and theoretical values being 3.50% and the largest difference in temperature in any data set of 23.0%. Further work is required to validate the entirety of the theoretical model, however the results obtained from the comparison between the theoretical and experimental data indicates that there is merit behind the rationale that was applied in the development of the theoretical model.

[1] K. E. Herold, R. Radermacher, S. A. Klein, Absorption Chillers and Heat Pumps, CRC Press, 1996.

[2] G. Grossman, A. Zaltash, ABSIM - modular simulation of advanced absorption systems, International Journal of Refrigeration 24 (2001) 531–543.

[3] C. Somers, A. Mortazavi, Y. Hwang, R. Radermacher, P. Rodgers, S. Al-Hashimi, Modeling water/lithium bromide absorption chillers in aspen plus, Applied Energy 88 (2011) 4197–4205.

[4] B. Bakhtiari, L. Fradette, R. Legros, J. Paris, A model for analysis and design of h2o-libr absorption heat pumps, Energy Conversion and Management 52 (2011) 1439–1448.

[5] P. Kohlenbach, F. Ziegler, A dynamic simulation model for transient absorption chiller performance. Part I: The model, International Journal of Refrigeration 31 (2008) 217–225.

[6] P. Kohlenbach, F. Ziegler, A dynamic simulation model for transient absorption chiller performance. part ii: Numerical results and experimental verification, International Journal of Refrigeration 31 (2008) 226–233.

[7] B. Kim, J. Park, Dynamic simulation of a single-effect ammonia-water absorption chiller, International Journal of Refrigeration 30 (2007) 535–545.

[8] Y. Shin, J. Seo, H. Cho, S. Nam, J. Jeong, Simulation of dynamics and control of a double-effect librh$_2$o absorption chiller, Applied Thermal Engineering 29 (2009) 2718–2725.

[9] G. Evola, N. Le Pierrès, F. Boudehenn, P. Papillon, Proposal and validation of a model for the dynamic simulation of a solar-assisted single-stage libr/water absorption chiller, International Journal of Refrigeration 36 (3) (2013) 1015–1028.

[10] J. Pátek, J. Klomfar, A computationally effective formulation of the thermodynamic properties of LiBr-H_2O solutions from 273 to 500 K over full composition range, International Journal of Refrigeration 29 (2006) 566–578.

[11] J. Pátek, J. Klomfar, Solid-liquid phase equilibrium in the systems of LiBr-H_2O and LiCl-H_2O, Fluid Phase Equilibria 250 (2006) 138–149.

[12] A. Mills, Heat Transfer, 2nd Edition, Prentice Hall, 1999.

[13] W. Wagner, J. R. Cooper, A. Dittmann, J. Kijima, H.-J. Kretzschmar, A. Kruse, R. Mares, K. Oguchi, H. Sato, I. Stocker, The IAPWS industrial formulation 1997 for the thermodynamic properties of water and steam, Journal of Engineering for Gas Turbines and Power (ASME) 122 (2000) 150–182.

[14] Y. A. Çengel, Heat Transfer: A Practical Approach, 2nd Edition, McGraw-Hill, 2003.

[15] J. D. Killion, S. Garimella, A critical review of models of coupled heat and mass transfer in falling-film absorption, International Journal of Refrigeration 24 (2001) 755–797.